CAMBRIDGE

Cambridge University Press & Assessment
978-1-605-11594-8 — Low-Dimensional Semiconductor Structures, Volume 1617
Edited by Tetyana V. Torchynska , Georgiy Polupan , Larysa Khomenkova , Gennadiy Burlak ,
Yuri V. Vorobiev , Zsolt J. Horvath
Excerpt
More Information

**III-V materials**

© in this web service Cambridge University Press & Assessment www.cambridge.org

CAMBRIDGE

Cambridge University Press & Assessment
978-1-605-11594-8 — Low-Dimensional Semiconductor Structures, Volume 1617
Edited by Tetyana V. Torchynska , Georgiy Polupan , Larysa Khomenkova , Gennadiy Burlak , Yuri V. Vorobiev , Zsolt J. Horvath
Excerpt
More Information

Mater. Res. Soc. Symp. Proc. Vol. 1617 © 2013 Materials Research Society
DOI: 10.1557/opl.2013.1156

# Electrical Properties of Quantum Wells in III-NITRIDE Alloys and the Role of Defects

Daniela Cavalcoli, Albert Minj, Saurabh Pandey, Beatrice Fraboni and Anna Cavallini
Physics and Astronomy Department, University of Bologna, Viale C Berti Pichat 6/II, I-40127 Bologna, Italy

## ABSTRACT

III-nitrides (III-Ns) semiconductors and their alloys have shown in the last few years high potential for interesting applications in photonics and electronics. III-Ns based heterostructures (HS) have been under wide investigation for different applications such as high frequency transistors, ultraviolet photodetector, light emitters etc. In the present contribution a III-Ns based heterostructure, in particular the nearly lattice matched $Al_{1-x}In_xN$/AlN/GaN HS will be discussed. The formation of the two dimensional electron gas (2DEG), its origin, its electrical and optical properties, the confined subband states in the well and its effect on the conduction mechanisms have been studied. Moreover, extended defects and their effect on the degradation phenomena of the 2DEG have been analyzed.

## INTRODUCTION

Notwithstanding the wide application range and interest in III-Nitride based heterostructures (HS), many material-related fundamental issues of these materials are still under investigation: interdiffusion of mobile species, In or Al incorporation or segregation [1,2] and the role of extended defects on the electrical properties [3-6] are still debated. As a case study of such heterostructures, the nearly lattice matched $Al_{1-x}In_xN$/AlN/GaN system will be here analyzed. This system has been studied only quite recently, as before 2005 very few data were available on these alloys, and high electron mobilities transistor were basically developed on AlGaN/GaN HS [7]. Later on, it was found that lattice-matched AlInN/GaN heterostructures exhibit more than twice the amount of electrons confined at the AlGaN/GaN heterointerface, and hence a serious interest arose in those HS for applications in high power electronics.

In $Al_{1-x}In_xN$/GaN HS, the strong band gap difference between AlN and $Al_{1-x}In_xN$ (with low In content, x around 0.13-0.14) and the very high polarization- induced electric field create a triangular potential well at the heterointerface, which is able to confine electrons, thus a two dimensional electron gas (2DEG) forms in the well. The electrons forming the 2DEG may suffer from poor in-plane transport properties due to alloy disorder induced scattering. To overcome this difficulty, the insertion of an AlN interlayer, an approach already explored within the AlGaN/GaN system, has been used. This helps to keep the electrons better confined in the GaN channel and prevents 2DEG electrons from alloy scattering. High carrier density (around $2\times10^{13}cm^{-2}$) and high mobility (around $2\times10^{3}$ $cm^2/Vs$) [7] are usually obtained in these structures. An example of such a well is sketched in fig1.

Notwithstanding the quite good structural and electrical properties of these structures, we have to remind here that III-Ns and their alloys suffer for the absence of suitable growth substrate. Sapphire is typically used, but thermal and lattice mismatch are responsible for the formation of threading dislocations (TDs) which start forming at the sapphire /GaN interface and propagate through the whole structure. Therefore, the study of the role of these defects on the transport properties of the HS is of the major importance. While structural properties of TDs have been widely investigated, electrical properties of TDs are still debated. As an example, III-Ns based HS show a quite intriguing “defect insensitivity”, which is still



© in this web service Cambridge University Press & Assessment www.cambridge.org

debated. III-Ns based HS are able to support, without strong degradation, a TD density considerably higher than III-Phosphorous based HS. The reason seems to be related to the strong ionicity of III-Ns, which places the surface states (as well as defect states) very close to the band edges, and to the existence of potential fluctuations in the band structures due to stacking faults, alloying phenomena and phase separation [8,9]. Both these phenomena would help preventing trap assisted electron-hole recombination. However, notwithstanding III-Ns based devices can tolerate a quite large defect density, the knowledge of the defect electrical characteristics and of their effect on the macroscopical electrical properties of the heterostructure is a fundamental issue that should be still widely explored.

The present contribution deals with a summary and a review of the results that we recently obtained on nearly lattice matched $Al_{1-x}In_xN$/AlN/GaN heterostructures with In content around 13%. These structures have been investigated by electrical macroscopical methods (current-Voltage, Hall effect), microscopical methods (Atomic Force Microscopy, in current and phase contrast mode) and spectroscopy techniques (Photovoltage, Photocurrent and Photoluminescence). The formation of the 2DEG, its electrical and optical properties, its origin and its role in the electrical conduction will be discussed. In addition, possible defect related degradation effects on the 2DEG properties will be discussed.

**EXPERIMENT**

Nearly lattice matched $Al_{1-x}In_xN$/AlN/GaN heterostructures were grown by AIXTRON and III-V lab by metal–organic chemical vapor deposition (MOCVD) on c-plane sapphire substrates. The nominal thickness of AlInN was varied as 15 and 30 nm, while the thickness of the AlN layer was varied between 0 and 2.5 nm. Indium content varies from 12.5% to 14.5% as assessed by high resolution X-ray diffraction (HR-XRD) [10]. Relaxed HS (with AlN thickness of 7.5 nm, above the critical thickness) were also studied. Further details on the sample growth can be found elsewhere [4,11].

Macroscopical electrical characterization has been carried out by Current-Voltage measurements either on back-to-back Schottky contacts in a planar configuration directly formed by In-Ga alloy with a spacing of 2mm, either on Ni-Au Schottky contacts (dots of 1 mm diameter) and Ti/Al/Ni/Au Ohmic contacts (dots of 0.6 mm diameter). Hall effect measurements were carried out at 77 and 300 K on Van der Pauw structures to obtain the 2DEG density and carrier mobility. Further details on these experimental procedures can be found in ref [4,12]. Spectroscopical analyses were carried out by Surface photo voltage spectroscopy (SPS) analyses were performed at room temperature by means of a custom-made apparatus based on Xenon lamp source and a SPEX 500M monochromator [13,14]. Photoluminescence measurements have been performed by exciting the carriers with 193 nm ArF excimer lasers with at 5 K. Photocurrent analyses have been performed in an Ohmic-Ohmic configuration on SiNx passivated samples.

Microscopic morphological and electrical analyses were obtained by AFM (NT MDT Solver PRO47) by using conductive probes (Pt-Ir, diamond, nanoneedles ($Ag_2Ga$-Nauganeedles LLC). Conductive AFM mapping and IV curves were obtained with the sample grounded [15]). The contact was made with conductive silver on one side of the sample piece.



© in this web service Cambridge University Press & Assessment www.cambridge.org

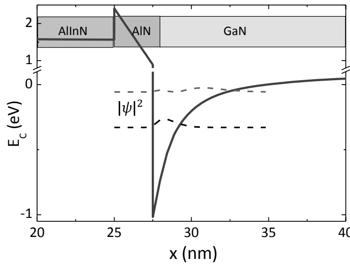


**Figure 1** Triangular potential well at the GaN/AlN interface. The well shape and the first two subband energy levels and wave functions are calculated from Schrödinger-Poisson solver for an AlN interlayer thickness of 2.5 nm. A sketch of the heterostructure is also shown.

## RESULTS

### 2DEG in $Al_{1-x}In_xN$/AlN/GaN heterostructures. Origin, electrical and optical properties.

AlN, GaN and AlInN possess polarized Wurtzite crystal structures, having dipoles across the crystal in the [0001] direction. In absence of external fields, spontaneous (pyroelectric) and strain induced (piezoelectric) polarizations contribute to the total macroscopic polarization [16]. In the AlInN/GaN system, this polarization induces an interface charge due to abrupt divergence in the polarization at the heterointerface. Even if the polarization is basically a volume effect, since vicinal dipole sheets in the z-direction cancel out each other, the polarization manifests itself mainly at interface as the difference of the total polarization of neighboring layers. Thin pseudomorphic AlN layers grown on GaN exhibit therefore a higher total polarization charge density due to the significant contribution of the piezoelectric polarization. In the case of lattice matched AlInN, this contribution vanishes completely and only the spontaneous polarization is present. If the polarization charge density is positive, electrons are attracted forming a 2DEG [7].

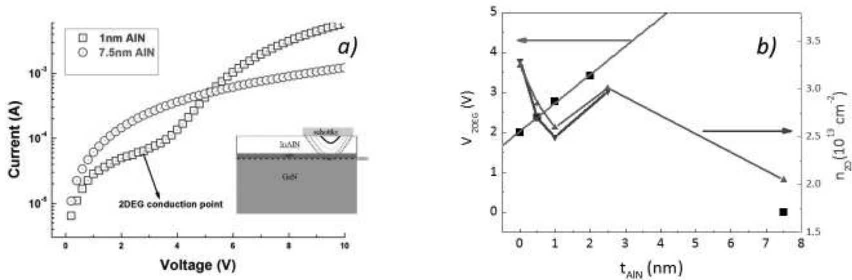


**Figure 2** (a) Current vs. Voltage plot showing slope change activating 2DEG conduction in samples with different AlN thickness. The depletion of reverse-biased Schottky with increasing bias is also shown (inset). (b) The bias activating 2DEG conduction $V_{2DEG}$ (left axis) and the 2DEG density $n_{2D}$ (right axis) are plotted as a function of the AlN interlayer thickness. Literature data have been plotted for comparison [12]. The last point (7.5nm) of our I-V curve has been extrapolated. The lines are a guide for the eye (reprinted from [12]).



© in this web service Cambridge University Press & Assessment www.cambridge.org

Figure 1 shows the band diagram structure of a nearly lattice matched AlInN/AlN/GaN HS and the position of the two subband states within the 2DEG channel, obtained by solving the 1-D Schroedinger-Poisson equation. Transport properties of the 2DEG in the HS are shown in figure 2. IV curves obtained on $Al_{1-x}In_xN$/AlN/GaN HS with AlN thickness ($t_{AlN}$ ) of 1 nm (below the critical thickness) and 7.5 nm (above the critical thickness, which is around 6.5 nm [17]) by back-to-back Schottky contacts in a planar configuration are shown in fig 2a. A clear change in the curve slope is visible in 1nm thick AlN samples, but not visible in 7.5nm AlN samples. The slope change occurs at an applied bias voltages which scale with the AlN thickness in different samples, except for the samples with a 7.5nm thick AlN interlayer (fig.2b). For low bias voltages the transport is limited to the top $Al_{1-x}In_xN$ barrier layer, as the applied bias voltage increases (fig. 2a inset), the depletion region extends further through the AlInN and AlN layers, allowing the current flow to reach the interface with the GaN substrate, where the 2DEG is located. The current increases when the conduction through the 2DEG is activated, apart from the sample with $t_{AlN}$=7.5 nm. In this sample large currents at very low bias voltages were observed, related to the presence of many TDs and nanocracks observed by AFM [3 and fig 5 below]. The $V_{2DEG}$ values were used to calculate the total effective polarization charge density, and by applying an electrostatic model [7], the 2DEG concentration, which is plotted in fig 2b as a function of $t_{AlN}$, and compared with literature data [12]. It can be noted that the transport properties of the 2DEG have been reliably investigated by macroscopic IV measurements.

The 2DEG density was evaluated also by microscopical IV analyses. The effect of the 2DEG on the local transport properties of the HS has also been investigated by C-AFM. We have demonstrated that current–voltage measurements performed with a conductive AFM tip on $Al_{1-x}In_xN$/AlN/GaN can be modeled by the thermionic emission from the 2DEG assisted by image-charge-induced barrier lowering. Other transport mechanisms that could be active in these heterostructures, such as tunneling or dislocation-assisted conduction mechanisms, have been ruled out due to the contact dimension (of the order of nanometers). The barrier lowering is caused by the image charge induced by the 2DEG and depends on the 2DEG characteristics. The 2DEG density can be thus be obtained by fitting the experimental data. The so obtained 2DEG density values have been found to be in very good agreement with the Hall measurements [15].

The optical properties of the 2DEG are of fundamental importance for optoelectronic device applications. Optically induced electronic transitions in AlInN/AlN/GaN HS with different In contents have been investigated by absorption (SPV and Photocurrent, PC) and emission spectroscopy (Photo Luminescence, PL). Figure 3a shows the possible electronic transitions in the HS as evaluated by solving Schrodinger-Pöisson equation, while figure 3b shows the direct measurement of these transitions. Energy level values of the subband states within the well at the GaN / AlN heterointerface have been measured by PL and PC as well, and the obtained results well compare with the simulated ones. Moreover, a strong enhancement of the Photoluminescence intensity due to holes recombining with electrons at the Fermi Energy, known as Fermi Energy Singularity (FES), has also been observed [14].

Another interesting point still under debate is the origin of the 2DEG. Surface donor states have been proposed to be the underlying cause of the 2DEG formation in the AlGaN layer [18]. Either a single surface state energy or a Fermi level pinning at the surface are able to explain the measured variation of the 2DEG concentration with the barrier thickness in AlGaN. By determining the Schottky barrier height in (Ni-Au)/ on $Al_{1-x}In_xN$/AlN/GaN Schottky diodes, measured by current-voltage (I-V) characteristics, we obtained the density and energy distribution of surface donor states.



© in this web service Cambridge University Press & Assessment www.cambridge.org

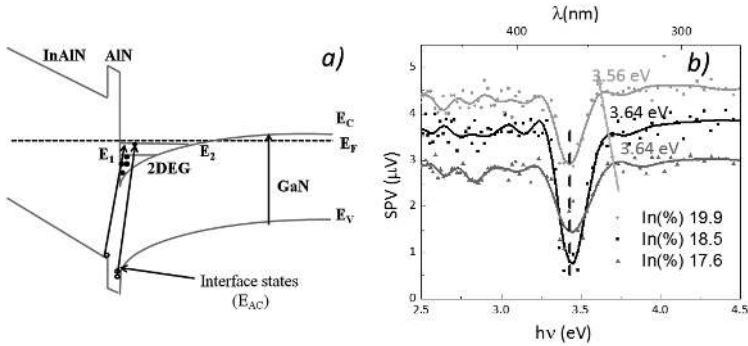


**Figure. 3 (a)** Schematic of the band structure for AlInN/AlN/GaN heterostructures calculated at 300 K from Schrodinger-Pöisson equation to show the possible photoexcited electronic transitions. **(b)** Surface Photovoltage signal plotted against photon energy for $Al_{1-x}In_xN$/AlN/GaN HS with different In content.

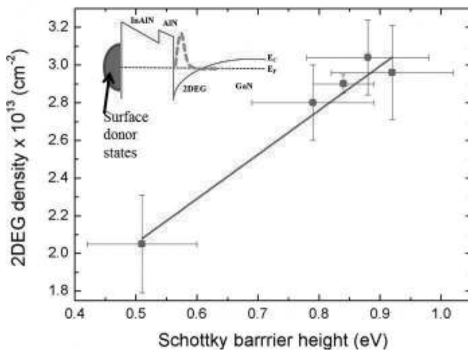


**Figure.4** 2DEG density as evaluated by Hall effect plotted as a function of the Schottky barrier height obtained by IV measurements of Schottky diode on AlInN/AlN/GaN HS.

Figure 4 shows that the 2DEG density, as measured by Hall effect in density in pseudomorphic $Al_{1-x}In_xN$/AlN/GaN HS, scales linearly with the Schottky barrier height. From the linear fit of the 2DEG density vs the barrier height, the value of the surface /interface donor density has been evaluated. The value of (2.7 ± 0.2) x $10^{13}$ $cm^{-2}$ $eV^{-1}$ was estimated [4]. The so-calculated value of surface donor density is in good agreement with earlier reports on AlGaN/GaN heterostructures [19, 20].

## Defect- related degradation phenomena of the 2DEG in $Al_{1-x}In_xN$/AlN/GaN Heterostructures

As already noted in the introduction, extended defects (threading dislocations, cracks..) and impurity segregation could induce degradation in the electrical and optical properties of the HS. Figure 5 shows AFM topographical micrographs of two $Al_{1-x}In_xN$/AlN/GaN HSs with different AlN interlayer thickness. The two structures exhibit a quite



© in this web service Cambridge University Press & Assessment www.cambridge.org

CAMBRIDGE
Cambridge University Press & Assessment
978-1-605-11594-8 — Low-Dimensional Semiconductor Structures, Volume 1617
Edited by Tetyana V. Torchynska , Georgiy Polupan , Larysa Khomenkova , Gennadiy Burlak , Yuri V. Vorobiev , Zsolt J. Horvath
Excerpt
More Information

different morphology, in the first case (fig 5a) a grain structure and V defects are visible, the V pit density in this sample ranges from $1x10^8$ to $5x10^8$ $cm^{-2}$ and the root mean square roughness around is around 0.23 nm, in the second case (fig 5b) several cracks appear, the V-pit density and roughness significantly increase from 0.1 to $3x10^{10}$ $cm^{-2}$ and 0.35 nm, respectively. V pit density and roughness values as a function of $t_{AlN}$ are shown in fig.6a. In segregation phenomena at TDs and cracks have been demonstrated by dynamical and current AFM analyses [2, 3], and have been shown to be the cause of enhanced conduction through TDs and cracks.

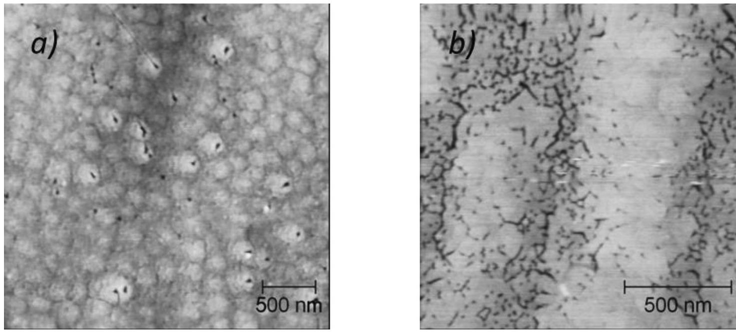


**Figure.5** AFM micrographs of AlInN/AlN/GaN HS with AlN layer thickness of 1 nm (a) and of 7.5 nm (b).

In order to analyze the effect of TDs and cracks on the macroscopical properties of the 2DEG, transport measurements were performed on pseudomorphic (AlN thickness up to to 2.5 nm) and to relaxed (AlN thickness 7.5 nm) structures. Hall effect mobility values measured at 77K are plotted as a function of the AlN thickness in figure5a. It is to be noted that mobility, as well as roughness and V-pit density, show a trend vs $t_{AlN}$. In order to identify the dominant scattering mechanisms controlling the low temperature electron mobility of the 2DEG, we have calculated the mobility related to different scattering mechanisms. The remote surface roughness (RSR) scattering mechanism explains the low temperature mobility in AlGaN/GaN and in AlN/GaN 2DEG channel layers, respectively [21, 22], while scattering due to dislocations, alloy disorder, phonons, etc., plays an important role in limiting the 2DEG room temperature mobility [22]. We evaluated the RSR controlled mobility inserting in the model morphological parameters (the correlation length) measured by AFM and STM (Scanning Tunnelling Microscopy), the dislocation controlled mobility using the V-pit density as evaluated by AFM and finally we combined the two contribution and evaluated the total mobility [11]. The total mobility has been thus calculated using measured amounts without any fitting parameters nor a priori assumptions. In fig 6b the dislocation related, RSR and total calculated mobilities are compared with the experimentally measured values and plotted *vs* the surface roughness. The good agreement between the experimental and calculated mobility values is evident for all the roughness values except for the highest one. Indeed, the last point corresponds to samples with interlayer thickness of 7.5 nm, in this case strain relaxation induces the formation of cracks piercing the 2DEG and thus creating electrical shunts (figure 5b) [3]. The 2DEG electrical transport in such sample should be strongly affected by those cracks which are not considered in the theoretical model. We can note from Fig. 6b that the RSR scattering mechanism is the most effective one in



© in this web service Cambridge University Press & Assessment www.cambridge.org

controlling the 2DEG mobility in $Al_{1-x}In_xN/AlN/GaN$ HS, as the dislocation related mobility does not play a major role.

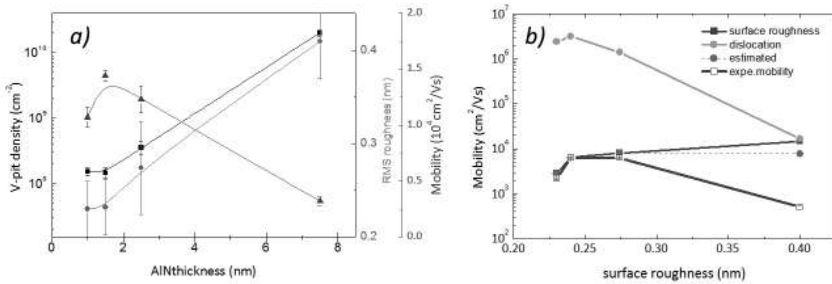


**Figure.6** **(a)** V pit density (black square), Root Mean Square Roughness (red dot) and Hall mobility (blue triangle) of AlInN/AlN/GaN HS as a function of AlN layer thickness. The HS are pseudomorphic for AlN thickness below 6.5 nm, relaxed above 6.5 nm. **(b)** Measured Hall effect mobility plotted vs the RMS roughness, compared with mobilities calculated by dislocation scattering (green dot) surface roughness (blue square) and total mobilities (red dot).

In order to study the effect of strain relaxation, TDs and cracks on the electrical properties of $Al_{1-x}In_xN/AlN/GaN$ HS, current-voltage measurements were performed at room temperature on Ni-Au Schottky contacts (dots of 1 mm diameter) and Ti/Al/Ni/Au Ohmic contacts (dots of 0.6 mm diameter). The ohmic and Schottky contacts were prepared by Ti/Al/Ni/Au and Ni-Au evaporation respectively; for ohmic metallization, further annealing was performed at 850 °C for 30 s in $N_2$ ambient. Forward and reverse bias current-voltage measurements performed at 300 K are shown in Fig. 7a. In the pseudomorphic HS, the reverse bias leakage current is reduced by increasing the AlN interlayer thickness from 0 nm up to 2 nm; while for the relaxed HS, where $t_{AlN}$ is 7.5 nm, the leakage current rapidly increases. The increase in the reverse bias leakage current could be related to the increase of the TD density, which is measured as V-pit density (fig.6a).

We have applied the Poole-Frenkel transport model [4] to interpret the leakage mechanisms in such AlInN/AlN/GaN HS, Poole-Frenkel emission refers to electric-field-enhanced thermal emission from a trap state into a continuum of electronic states. In the present case the trap states can be dislocation related. In fig. 7b we have plotted I/E vs $E^{1/2}$ and found for the pseudomorphic structures a linear dependence in the log scale as predicted by Poole Frenkel mechanism. These results indicate that the Poole-Frenkel mechanism is the dominant mechanism controlling the reverse leakage current in AlInN/GaN nearly lattice matched heterostructures. for the relaxed structure with 7.5 nm thick AlN layer, the current becomes nearly independent of $E^{1/2}$ suggesting that other mechanisms, such for example conduction through electrically active nanocracks, could play a major role.



© in this web service Cambridge University Press & Assessment www.cambridge.org

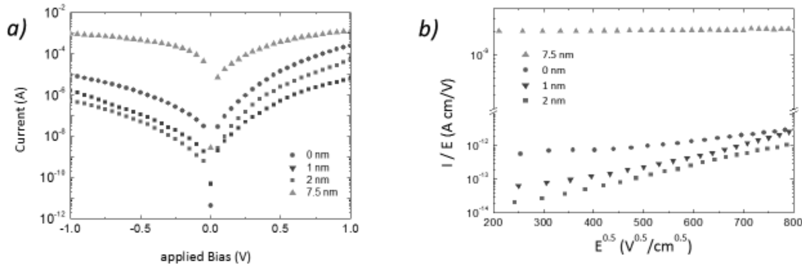


**Figure 7.** (a) IV curves showing the variation of reverse bias leakage current with different AlN interlayer thickness. (b) Measured reverse-bias current divided by electric field vs square root of electric field for Schottky contact on the $Al_{1-x}In_xN$/AlN/GaN heterostructure

## DISCUSSION AND CONCLUSIONS

The aim of the present contribution is to review the results obtained by the present authors on III-nitride based heterostructures, in particular on $Al_{1-x}In_xN$/AlN/GaN HS with different AlN layer thickness. At the heterointerface between $Al_{1-x}In_xN$/AlN/GaN a 2DEG forms. We have described the formation of the 2DEG, its origin, the analysis of its electrical and optical characteristics . Furthermore, we have investigated degradation effects of the HS and related them to defective states and morphological properties investigated at the nanoscale by AFM.

We have demonstrated that the 2DEG plays a fundamental role on the electrical and optical properties of the HS and that threading dislocations, cracks, and impurity decorated defects play a strong role on the degradation mechanisms of $Al_{1-x}In_xN$/AlN/GaN heterostructures.

## ACKNOWLEDGMENTS

H. Behmenburg, C. Giesen and M. Heuken of Aixtron SE, Herzogenrath, Germany, and P. Gamarra, and M. A. Poisson, of III-V lab, France, are gratefully acknowledged for providing the samples and for the useful discussion. T Brazzini from ISOM, ETSI Telecomunicación, Universidad Politécnica de Madrid, is gratefully acknowledged for Schottky diode preparation. D. Skuridina, P. Vogt, M. Kneissl of the Technical University of Berlin are gratefully acknowledged for useful discussion and support in STM experiments.
This work was supported by the EU under Project No. PITN-GA-2008 213238-RAINBOW.



© in this web service Cambridge University Press & Assessment www.cambridge.org

CAMBRIDGE

Cambridge University Press & Assessment
978-1-605-11594-8 — Low-Dimensional Semiconductor Structures, Volume 1617
Edited by Tetyana V. Torchynska , Georgiy Polupan , Larysa Khomenkova , Gennadiy Burlak , Yuri V. Vorobiev , Zsolt J. Horvath
Excerpt
More Information

**REFERENCES**

1. Th Kehagias et al. Appl. Phys. Lett. **95**, 071905 (2009).
2. A. Minj, D. Cavalcoli, A. Cavallini, Appl. Phys. Lett., **97**, 132114 (2010).
3. A. Minj, D. Cavalcoli, S. Pandey, B. Fraboni, A. Cavallini, T. Brazzini, F. Calle Script Mater, **66** 327 (2012).
4. S. Pandey, D. Cavalcoli, B. Fraboni, A. Cavallini, T. Brazzini, and F. Calle Appl. Phys. Lett.**100**, 152116 (2012).
5. F. A. Ponce, Ann. Phys. (Berlin), **1 – 2,** 523 75 (2011)
6. D. C. Look and J. R. Sizelove, Phys. Rev. Lett. **82**, 1237 (1999).
7. M Gonschorek, et al International Journal of Microwave and Wireless Technologies, , 2(1), 13–20 (2010).
8. S. F. Chichibu et al, Nature Materials **810-816** (2006)
9. T.D Moustakas Phys. Status Solidi A **210**, 1, 169–174 (2013)
10. Vilalta-Clemente A, Poisson M-A, Behmenburg H, Giesen C, Heuken M and Ruterana Phys. Status Solidi a **207** 1105 (2010)
11. S. Pandey, D. Cavalcoli, A. Minj, B. Fraboni, A. Cavallini, D. Skuridina, P. Vogt, M. Kneissl Acta Materialia **60** 3176–3180 (2012)
12. S Pandey, B Fraboni, D Cavalcoli, A Minj, A Cavallini - Applied Physics Letters, **99**, 012111 (2011)
13. D Cavalcoli, S Pandey, B Fraboni, A Cavallini Appl Phys Lett **98** 142111-142111(2011).
14. S. Pandey, D. Cavalcoli, A. Minj, B. Fraboni, A. Cavallini et al. J. Appl Phys. **112**, 123721 (2012)
15. A. Minj, D Cavalcoli and Anna Cavallini Nanotechnology **23** (2012) 115701
16. I. P. Smorchkova et al Appl. Phys. **86,** 4520 (1999)
17. M. Gonschorek et al J. of Appl Phys **103**, 093714 (2008)
18. A Rizzi et al Appl. Phys. A **87**, 505–509 (2007)
19. G. Koley, M. G. Spencer, Appl. Phys. Lett. **86**, 042107 (2005).
20. M. S. Miao, A. Janotti, C. G. Van de Walle, Phys. Rev. B **80**, 155319 (2009).
21. B. Liu et al Appl. Phys. Lett. **97**, 262111 (2010)
22. Y. Cao and D. Jena, Appl. Phys. Lett. **97**, 222116 (2010)



© in this web service Cambridge University Press & Assessment www.cambridge.org